PNAS

Supporting Information for

Thermoelectricity at a gallium-mercury liquid metal interface

Marlone Vernet, Stephan Fauve and Christophe Gissinger

Corresponding Author: Christophe Gissinger
E-mail: christophe.gissinger@phys.ens.fr

This PDF file includes:

Supporting text
Figs. S1 to S6
Legend for Movie S1

Other supporting materials for this manuscript include the following:

Movie S1

Supporting Information Text

Sidewall convection

The presence of horizontal temperature gradient naturally leads to sidewall convection which appears at non-zero ΔT_0. The Rayleigh number $Ra = \alpha \Delta T_0 \Delta R^3 / \kappa \nu$ where α is the thermal expansion coefficient, ΔT_0 the temperature difference between the cylinders, $\Delta R = R_o - R_i$, κ the thermal diffusivity and ν the kinematic viscosity. For liquid Gallium, $\alpha = 5.5 \cdot 10^{-5}\ K^{-1}$, $\kappa = 1.3 \cdot 10^{-5}\ m^2.s^{-1}$, $\nu = 3.18 \cdot 10^{-7}\ m^2.s^{-1}$. The Rayleigh number for $\Delta T_0 \sim 2 - 37\ K$ is $Ra_{Ga} \sim 5.7 \cdot 10^3 - 1.06 \cdot 10^5$. For liquid Mercury, $\alpha = 1.83 \cdot 10^{-4}\ K^{-1}$, $\kappa = 4.9 \cdot 10^{-6}\ m^2.s^{-1}$, $\nu = 1.49 \cdot 10^{-7}\ m^2.s^{-1}$. The Rayleigh number for $\Delta T_0 \sim 2 - 37\ K$ is $Ra_{Hg} \sim 1.08 - 20.03 \cdot 10^5$.

Analytical model

We derive here a simple analytical model describing the generation of a thermoelectric current, the corresponding magnetic field, and electric potential, in a rectangular domain made of two dissimilar metals. The two electrically conducting regions, denoted by the indices $'+'$ or $'-'$, have electrical conductivity $\sigma^{\pm}$ and Seebeck coefficient (or thermoelectric power) $S^{\pm}$. Both are supposed independent of temperature. A horizontal thermal gradient of arbitrary shape is applied across the two metals, which are separated by an electrically conducting interface located at $z = 0$.

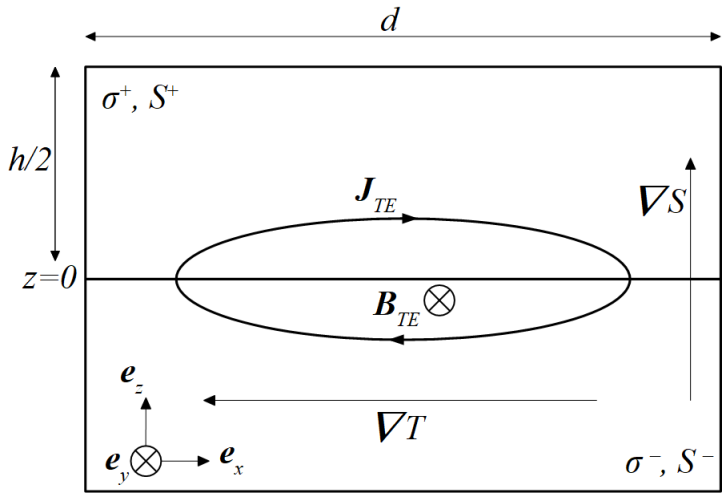

Fig. S1. Two metals with Seebeck coefficients $S^{\pm}$ and electrical conductivities $\sigma^{\pm}$, superimposed in a rectangular closed domain, are in electrical contact at $z = 0$, and subjected to a horizontal temperature gradient.

In the absence of a velocity field $\boldsymbol{u}$ and in the presence of a thermal gradient, Ohm's law reads:

$$\frac{\boldsymbol{j}}{\sigma} = \boldsymbol{E} - S \boldsymbol{\nabla} T, \qquad [1]$$

where $\boldsymbol{j}$ is the electric current density, σ is the electrical conductivity, $\boldsymbol{E}$ is the electric field, S is the Seebeck coefficient and T is the temperature field.

In the following we will use the magnetostatic approximation, relatively well satisfied here: in liquid metal, the magnetic field generally evolves on time scales much smaller than all the other variables such as the temperature or the velocity field. This is summed up by the dimensionless number $\zeta = \mu_0 \sigma \kappa$, with μ_0 the vacuum magnetic permeability. ζ is the ratio of the temperature evolution time scale due to thermal diffusion to the magnetic evolution time scale (also due to diffusion). The presence of convection implies that the temperature can evolve on time scale faster than $\Delta R^2 / \kappa$ like the eddy turnover time, $\Delta R / U_{ff}$ and U_{ff} being a typical velocity scale due to convection such as the free-fall velocity $U_{ff} \sim \sqrt{\alpha \Delta T_0 g h}$. In that case, $Rm = \mu_0 \sigma U_{ff} \Delta R$ must also be small to fulfill the quasi-static approximation. In the present experiment, both $\zeta \ll 1$ and $Rm \ll 1$, ensure that the evolution of the magnetic field produced by thermoelectricity follows adiabatically the evolution of temperature.

In the magnetostatic approximation and for steady state, the Maxwell-Faraday equation reads $\boldsymbol{\nabla} \times \boldsymbol{E} = 0$. For each layer, the electric field can then be decomposed as follows, $\boldsymbol{E} = -\boldsymbol{\nabla} V^{\pm}$ where $V^{\pm}$ is the electric potential in each subdomain.

Taking the curl of the Ohm's law (1) in each subdomain:

$$\nabla \times \left(\frac{\boldsymbol{j}^{\pm}}{\sigma^{\pm}} \right) = -\nabla \times (S \boldsymbol{\nabla} T) = \boldsymbol{\nabla} S \times \boldsymbol{\nabla} T \quad [2]$$

Because $S(T)$ is a function of temperature only, $\boldsymbol{\nabla} S \times \boldsymbol{\nabla} T = 0$. With the assumption that the electrical conductivity is constant in each domain, we get :

$$\boldsymbol{j}^{\pm} = -\sigma^{\pm} \boldsymbol{\nabla} \phi^{\pm} \quad [3]$$

The charge conservation, in the magnetostatic approximation, implies $\boldsymbol{\nabla} \cdot \boldsymbol{j}^{\pm} = 0$. Therefore, in each domain, $\phi^{\pm}$ fulfills a Laplace equation $\nabla^2 \phi^{\pm} = 0$. The boundary conditions for the current are prescribed by charge conservation:

$$j_x^{\pm}(x = 0, z) = j_x^{\pm}(x = d, z) = 0, \quad [4]$$

$$j_z^{+}(x, z = h/2) = j_z^{-}(x, z = -h/2) = 0, \quad [5]$$

$$j_z^{+}(x, z = 0^{+}) = j_z^{-}(x, z = 0^{-}) \quad [6]$$

These boundary conditions can be translated for $\phi^{\pm}$ as:

$$\partial_x \phi^{\pm}(x = 0, z) = \partial_x \phi^{\pm}(x = d, z) = 0, \quad [7]$$

$$\partial_z \phi^{+}(x, z = h/2) = \partial_z \phi^{-}(x, z = -h/2) = 0, \quad [8]$$

$$\sigma^{+} \partial_z \phi^{+}(x, z = 0^{+}) = \sigma^{-} \partial_z \phi^{-}(x, z = 0^{-}) \quad [9]$$

The quantity $\phi^{\pm}$ can then be obtained as a decomposition over the eigenfunctions of the Laplacian. It is clear that $\sin(n\pi x/d)$, with $n \in \mathbb{N}$, fulfill the boundary conditions for $\partial_x \phi^{\pm}$, thus

$$\phi^{\pm} = \sum_n \cos\left(\frac{n\pi x}{d} \right) g_n^{\pm}(z). \quad [10]$$

As $\phi^{\pm}$ respects a Laplace equation, it is easy to check that $g_n^{\pm}(z) = a_n^{\pm} \cosh(\kappa_n z) + b_n^{\pm} \sinh(\kappa_n z)$ with $\kappa_n = n\pi/d$ for simplicity. The boundary conditions at $z = \pm h/2$ then implies:

$$\frac{dg_n^{\pm}}{dz}(z = \pm h/2) = \kappa_n a_n^{\pm} \sinh(\pm \kappa_n h/2) + \kappa_n b_n^{\pm} \cosh(\pm \kappa_n h/2) = 0, \quad [11]$$

which is a constraint on the coefficients since $b_n^{\pm} = \mp \tanh(\kappa_n h/2) a_n^{\pm}$. Injected in $\phi^{\pm}$, it gives:

$$\phi^{\pm} = \sum_n a_n^{\pm} \cos(\kappa_n x)(\cosh(\kappa_n z) \mp \tanh(\kappa_n h/2) \sinh(\kappa_n z)). \quad [12]$$

Finally, the boundary condition at $z = 0$ for $\phi^{\pm}$ links the coefficients a_n^{+} and a_n^{-}. Indeed, it is easy to check that $a_n^{-} = -\sigma^{+} a_n^{+}/\sigma^{-}$. The continuity of the electric potential at the interface between the two conductors gives:

$$V^{+}(x, z = 0^{+}) - V^{-}(x, z = 0^{-}) = 0, \quad [13]$$

Using the Ohm's law $\boldsymbol{\nabla} V^{\pm} = \boldsymbol{\nabla}(\phi^{\pm} - S^{\pm} T)$ where S is considered constant in each phase, the previous expression can be recast in terms of $\phi^{\pm}$:

$$\phi^{+}(x, z = 0^{+}) - \phi^{-}(x, z = 0^{-}) = \Delta S T(x, 0), \quad [14]$$

with $\Delta S = S^{+} - S^{-}$. Injecting the expression of ϕ^{+} and ϕ^{-} gives:

$$\sum_n a_n^{+} \frac{\sigma^{+} + \sigma^{-}}{\sigma^{-}} \cos(\kappa_n x) = \Delta S T(x, z = 0), \quad [15]$$

multiplying this expression by $\cos(\kappa_m x)$ and integrating over the interval $[0, d]$ enables to obtain the expression of a_n^{+} (where the orthogonality relation for trigonometric function has been used):

$$a_n^{+} = \frac{K_n \sigma^{-} \Delta S}{d(\sigma^{+} + \sigma^{-})} \int_0^d T(x, 0) \cos(\kappa_n x) dx. \quad [16]$$

with $K_n = 1$ if $n = 0$ and $K_n = 2$ otherwise. Finally, this gives the potential:

$$\phi^{\pm} = \pm \sum_n \frac{K_n \sigma^{\mp} \Delta S}{d(\sigma^{+} + \sigma^{-})} \cos(\kappa_n x)(\cosh(\kappa_n z) \mp \tanh(\kappa_n h/2) \sinh(\kappa_n z)) \int_0^d T(x, 0) \cos(\kappa_n x) dx. \quad [17]$$

The potential ϕ which prescribes the thermoelectric current distribution is therefore completely determined by the temperature profile at the interface. The computation of $\boldsymbol{j}^{\pm}$ and $\boldsymbol{B}$ which is given by Maxwell-Ampère law's $\boldsymbol{\nabla} \times \boldsymbol{B} = \mu_0 \boldsymbol{j}$, is straightforward:

$$j_x^{\pm} = \pm \sum_n \frac{K_n \tilde{\sigma} \Delta S \kappa_n}{d} \sin(\kappa_n x)(\cosh(\kappa_n z) \mp \tanh(\kappa_n h/2) \sinh(\kappa_n z)) I_n(T), \quad [18]$$

$$j_z^{\pm} = \mp \sum_n \frac{K_n \tilde{\sigma} \Delta S \kappa_n}{d} \cos(\kappa_n x)(\sinh(\kappa_n z) \mp \tanh(\kappa_n h/2) \cosh(\kappa_n z)) I_n(T), \quad [19]$$

with $\tilde{\sigma} = \sigma^+ \sigma^- / (\sigma^+ + \sigma^-)$ and $I_n(T) = \int_0^d T(x,0) \cos(\kappa_n x) dx$. The important point of this result is the fact that any variation of the temperature along z will be supported by V keeping ϕ, $\boldsymbol{j}$, and $\boldsymbol{B}$ unchanged. The component of the magnetic field produced by the thermoelectric effect is orthogonal to the plane (x, z), B_y simply denoted B and is:

$$B^{\pm} = \mp \sum_n \frac{K_n \mu_0 \tilde{\sigma} \Delta S}{d} \sin(\kappa_n x)(\sinh(\kappa_n z) \mp \tanh(\kappa_n h/2) \cosh(\kappa_n z)) I_n(T), \quad [20]$$

We now implement this expression using the geometry and properties of the metals used in the experiment, namely mercury and gallium, $h = 25$ mm, $d = 60$ mm. If the two metals were in a solid state, the temperature profile would be linear with a constant thermal gradient $-\Delta T_0/d$, where ΔT_0 is the thermal gradient applied at the horizontal wall boundaries. Fig. S2 shows the computed isoline of potential $\phi^{\pm}$ while Fig. S3 shows a colormap of B for $n_{max} = 400$, using the value $\Delta T_0 = 37$K obtained in the experiment at maximum heating power. The black lines correspond to the streamlines of the thermoelectric current. The resolution used to plot the solution is $dx = 5 \cdot 10^{-4} d$ and $dz = 5 \cdot 10^{-4} h$.

In the more realistic case of an interface separating two liquid metals, as in the experiment, the temperature profile can be approximated as piecewise linear at the interface. Here again, we use the temperatures obtained in the experiment (the red profile shown in Fig.2 of the main text). The resulting solution is shown in Fig S4 and Fig S5. The results are in excellent agreement with those obtained from the direct numerical simulations reported in the main manuscript, and confirm the existence of intense current loops near the boundaries and a saddle point at the interface.

Fig. S6 shows the horizontal component of the thermoelectric current at $z = +0.5mm$ for the two cases studied. Far enough from the vertical walls, a good estimate of j_x in the solid case is $\tilde{\sigma} \Delta S \Delta T_0 / d$ while for the liquid case, $\tilde{\sigma} \Delta S \Delta T_B / d$ provides the correct estimate, in agreement with numerical predictions.

This agreement between theoretical predictions and numerical results confirms that the geometry of thermoelectric currents and magnetic field strength are controlled by the temperature profile at the interface, $\tilde{\sigma}$ and ΔS. This also confirms that the liquid nature of the interface, which produces a complex non-linear temperature profile, can generate a non-trivial distribution of thermoelectric currents, particularly near the thermal boundaries.

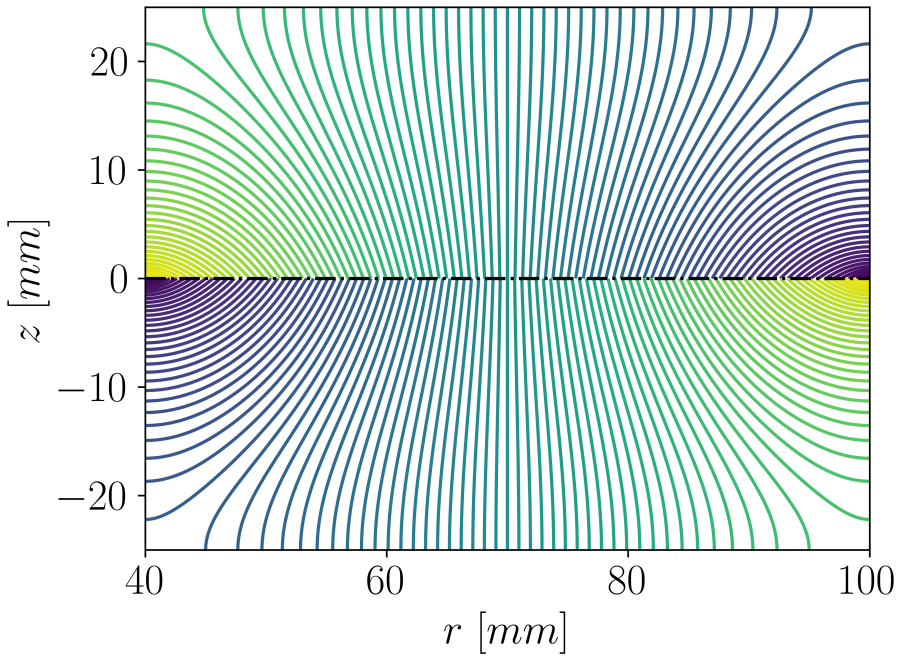

Fig. S2. Line of potential ϕ in the cartesian domain $[0, d] \times [-h/2, h/2]$. The dashed-dotted line corresponds to the position of the interface. The temperature profile at the interface displays a linear gradient, corresponding to the case where at least one of the metals is solid.

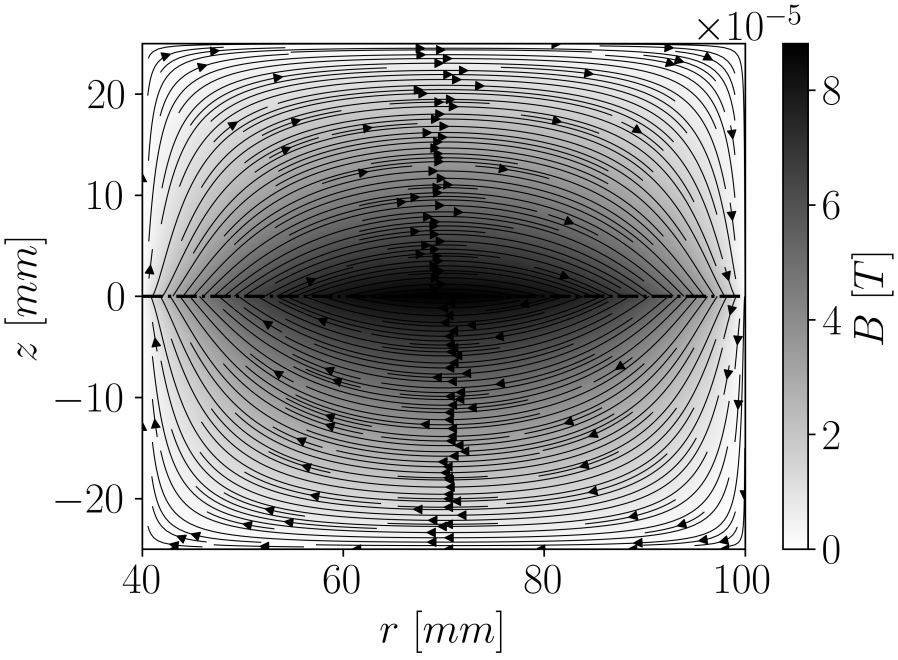

Fig. S3. Colormap of the magnetic field B in the cartesian domain $[0, d] \times [-h/2, h/2]$. The dashed-dotted line corresponds to the position of the interface. The black lines are the electric current. The temperature profile at the interface displays a linear gradient, corresponding to the case where at least one of the metals is solid.

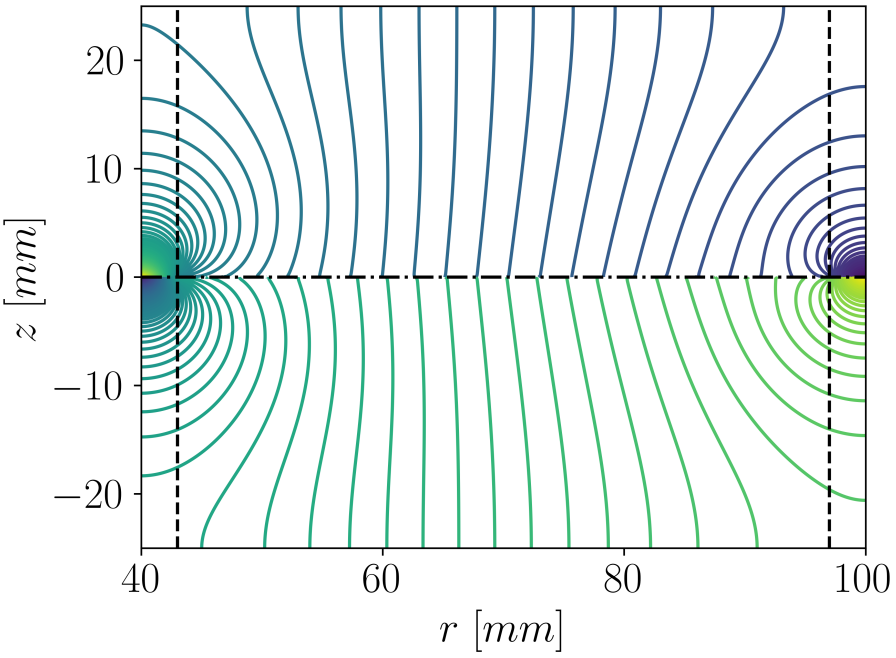

Fig. S4. Line of potential ϕ in the cartesian domain $[0, d] \times [-h/2, h/2]$. The dashed-dotted line corresponds to the position of the interface. The temperature profile at the interface is a piecewise linear gradient, and the vertical dashed lines indicate the positions of the thermal boundary layers..

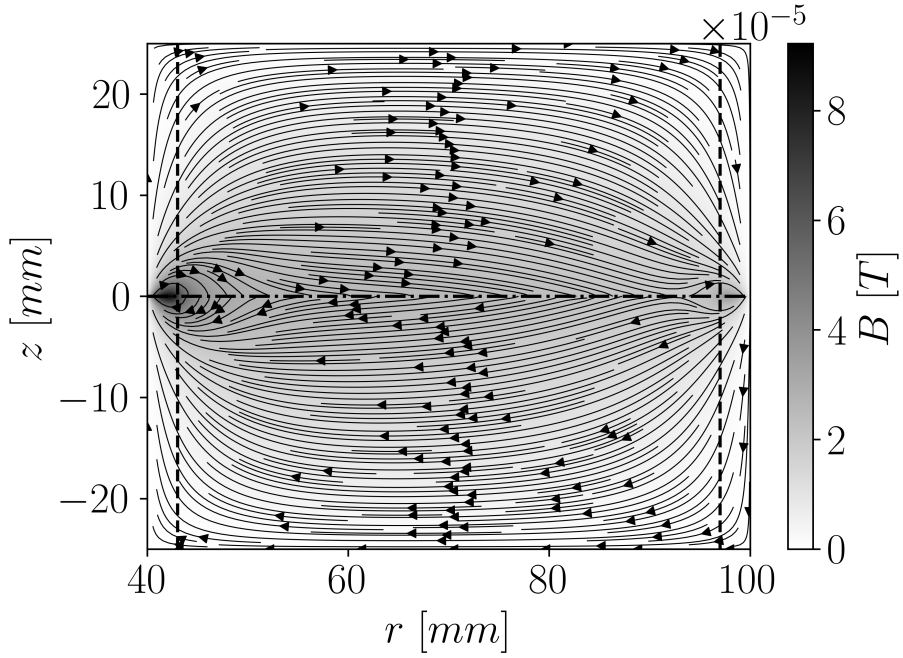

Fig. S5. Colormap of the magnetic field B in the cartesian domain $[0, d] \times [-h/2, h/2]$. The dashed-dotted line corresponds to the position of the interface. The black lines are the electric current. The temperature profile at the interface is a piecewise linear gradient, and the vertical dashed lines indicate the positions of the thermal boundary layers.

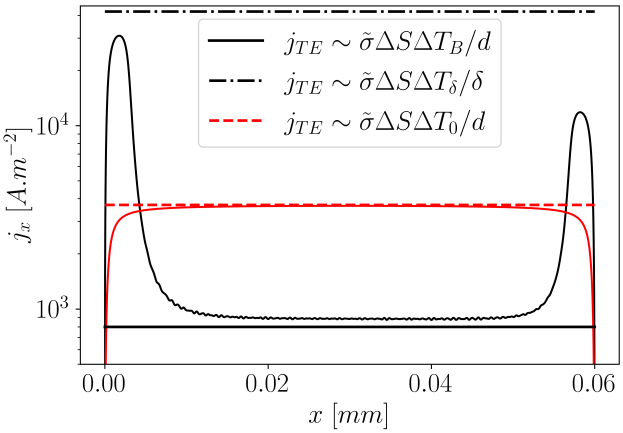

Fig. S6. Comparison between the horizontal component of the thermoelectric current density for a solid (red line) and a liquid interface (black line) both taken at $z = +0.5mm$.

Movie S1. Movie showing a typical experiment without top endcap, obtained for $\Delta T_0 = 37K$ and $B_0 = 36mT$. The strong thermoelectric forcing in the bulk causes the fluid to move azimuthally at the interface, with abnormally high velocities near the boundaries where the thermoelectric current is large.